Absolute Cross Section from van der Meer Scan

Zhangbu Xu,(2) Richard Majka,(2) Jack Sandweiss(2)

(The STAR Collaboration)

Angelika Drees,(1)

(1) *Brookhaven National Laboratory, Upton, New York 11973*

(2) *Physics Department, Yale University, New Haven, CT 06520*

(October 9, 2000)

We measure the absolute cross section seen by ZDC coincidences using the van der Meer Scan (Vernier Scan) at the STAR interaction point (IP). RHIC beam position monitors and results from STAR tracking vertex are found to be consistent. The absolute cross section of Au+Au at $\sqrt{s_{NN}} = 130GeV$ is determined to be $8.9{\pm}0.34(stat){\pm}0.51(sys)$(barn). Comparison with theoretic prediction is presented. The result is used to normalize the $d\sigma_{Au+Au}/dN_{ch}$ measured by STAR TPC.

STAR internal note

I. INTRODUCTION

The interaction cross section as function of transverse energy E_T or charge multiplicity N_{ch} is one of the necessary global event features for specifying the parameters of the initial state in relativistic heavy ion collisions [1]. In this note, we describe in detail the method of measuring the absolute cross section of Au+Au at $\sqrt{s_{NN}} = 130GeV$ and the normalization applied to $d\sigma_{Au+Au}/dN_{ch}$ measured by STAR TPC at RHIC. Because STAR used ZDC coincidences (Zero Degree Calorimeter) [2,3] as a minbias trigger, the total absolute cross section presented here is the total cross section seen by the ZDC coincidences from Au+Au interactions which include minbias nuclear interactions and mutual Coulomb Dissociation [2]. Details of the unnormalized dN/dN_{ch} are described elsewhere.

Since RHIC is a collider, we use the van der Meer Scan (also known as Vernier Scan) to determine the luminosity and absolute cross section. In the next few sections, we will give some basics on the Vernier Scan, the measurements of all the parameters required in luminosity and absolute cross section calculations. Section (II) describes the formulae for luminosity and cross section. Section (III) presents the details of the measurements and error estimates. Section (VI) deals with beam-gas events, primary vertex efficiency and some understanding of ZDC trigger and geometric acceptance and comparison with theory.

II. VAN DER MEER SCAN

The van der Meer Scan was invented by S. van der Meer in 1968 [4] who showed that it is possible to measure the effective height h_e of the colliding ISR beams by observing the counting rate R in a suitable monitor system while sweeping the two beams vertically through each other. "A bell-shaped curve will result with its maximum at zero displacement. It will now be shown that, irrespective of beam shape, h_e is equal to the area under this curve, divided by the ordinate for zero displacement ($h_e^\star$)." [4] At the ISR, the interaction point (IP) is defined by crossing two beams at angle α since the beams were not bunched. Luminosity is therefore defined as:

$$L = \frac{I_1 I_2}{e^2 c h_e tg(\frac{1}{2}\alpha)} \tag{1}$$

where e = charge on electron, c = velocity of light and I_1 and I_2 are beam currents [4–6]. h_e is :

$$h_e = \frac{\int \rho_1(z)dz \times \int \rho_2(z)dz}{\int \rho_1(z) \times \rho_2(z)dz} \tag{2}$$

where $\rho(z)$ is the beam density perpindicular to beam plane. It was demonstrated [4] or can be easily demonstrated that

$$h_e^\star = \frac{\int [\int \rho_1(z) \times \rho_2(z-x)dz]dx}{\int \rho_1(z) \times \rho_2(z)dz}$$

$$= \frac{\int [\int \rho_1(z) \times \rho_2(z-x)dx]dz}{\int \rho_1(z) \times \rho_2(z)dz}$$

Replacing the finite integral $\int \rho_2(z-x)dx$ with $\int \rho_2(z)dz$, we have

$$h_e^\star = h_e$$

With this method, the error of the measurements of the absolute cross section at the ISR was determined to be $\lesssim 1\%$ [5,6].

At RHIC, the beams are bunched and cogged with zero crossing angle at the IP. Here, we will follow [7] to present the relations between luminosity, cross section, effective area from Vernier Scan and the interaction area seen by detector.

The interaction rate N_{ZDC} is defined as the numbers of the beam particles (N_{b1} and N_{b2}) going through each other in some area A with cross section σ or

$$N_{ZDC} = \frac{N_{b1}N_{b2}}{A}\sigma = L\sigma \tag{3}$$

For two beams (Blue and Yellow in our case) with Gaussian distribution $\rho(x,y)$ in both horizontal and vertical directions, we have the luminosity as:

$$L = k_b f_{rev} \int_{-\infty}^{+\infty} \int_{-\infty}^{+\infty} \rho_1(x,y)\rho_2(x,y)dxdy \tag{4}$$

where k_b is number of bunches in a beam, f_{rev} is the revolution frequency ($7.8 \times 10^4 Hz$),

$$\rho_i = N_i \frac{1}{\sqrt{2\pi}\sigma_{xi}} \exp\left[-\frac{x^2}{2\sigma_{xi}^2}\right] \frac{1}{\sqrt{2\pi}\sigma_{yi}} \exp\left[-\frac{y^2}{2\sigma_{yi}^2}\right] \tag{5}$$

with i=1,2 for blue and yellow beams respectively and N_i are number of particles per bunch assuming all bunches in one beam are the same. Bunch variation will be discussed in an other section. Integrating over x and y, the luminosity is given by

$$L = \frac{k_b f_{rev} N_1 N_2}{2\pi\sqrt{(\sigma_{x1}^2 + \sigma_{x2}^2)(\sigma_{y1}^2 + \sigma_{y2}^2)}} \tag{6}$$

For beams not centered, consider the case of one beam displaced by d in the X direction, we have:

$$\rho_1 = N_1 \frac{1}{\sqrt{2\pi}\sigma_{x1}} \exp\left[-\frac{(x-d)^2}{2\sigma_{x1}^2}\right] \frac{1}{\sqrt{2\pi}\sigma_{y1}} \exp\left[-\frac{y^2}{2\sigma_{y1}^2}\right] \tag{7}$$

Reintegrating Eq.4 with the modified ρ_1, the luminosity $L(d)$ as function of d is

$$L(d) = \frac{k_b f_{rev} N_1 N_2}{2\pi\sqrt{(\sigma_{x1}^2 + \sigma_{x2}^2)(\sigma_{y1}^2 + \sigma_{y2}^2)}} \exp\left[-\frac{d^2}{2(\sigma_{x1}^2 + \sigma_{x2}^2)}\right] \tag{8}$$

The peak of the beam position with the displacement of d becomes

$$\bar{x} = \frac{d}{1 + \sigma_{x1}^2/\sigma_{x2}^2} \tag{9}$$

From Eq.8 and Eq.6, we see that the width of the Gaussian distribution from Vernier Scan is the width required in luminosity calculation! We have demonstrated that beam profile from van der Meer Scan (σ_{Vx}, σ_{Vy}) is the beam profile we want to put into the luminosity calculation.

This beam profile we see when we use the TPC tracking ($\sigma_{tpcx}, \sigma_{tpcy}$) to reconstruct the beam dimensions is given by the differential luminosity or interaction rate at (x,y), we get the following from Eq.4

$$L(x,y) = k_b f_{rev} \rho_1(x,y)\rho_2(x,y) = \frac{k_b f_{rev} N_1 N_2}{(2\pi)^2 \sigma_{x1}\sigma_{x2}\sigma_{y1}\sigma_{y2}} \exp\left[-\frac{x^2}{2}\left(\frac{1}{\sigma_{x1}^2} + \frac{1}{\sigma_{x2}^2}\right)\right] \exp\left[-\frac{y^2}{2}\left(\frac{1}{\sigma_{y1}^2} + \frac{1}{\sigma_{x2}^2}\right)\right] \tag{10}$$

From this, we now have the relation between different beam profile definitions,

$$\sigma_{Vx} = \sqrt{\sigma_{x1}^2 + \sigma_{x2}^2} \tag{11}$$

$$\sigma_{tpcx} = \frac{\sigma_{x1}\sigma_{x2}}{\sqrt{\sigma_{x1}^2 + \sigma_{x2}^2}} \tag{12}$$

If two beams have same size $\sigma_{x1} = \sigma_{x2} = \sigma_x$, we get:

$$\sigma_{Vx} = \sqrt{2}\sigma_x, \sigma_{tpcx} = \sigma_x/\sqrt{2}, \bar{x} = d/2 \tag{13}$$

Because we measure the effective beam area over the whole longitudinal interaction range instead of measuring the beam transverse size at the IP zero, the bunch length correction [8] is taken into account automatically.

We can go one step further and ask what will happen if the horizontal and vertical axes which we do the scans are not the principal axes of the beam ellipse. With some simple Algebra, we get:

$$\sigma_{Vx} = \sqrt{\frac{(\sigma_{x1}^2 + \sigma_{x2}^2)(\sigma_{y1}^2 + \sigma_{y2}^2)}{(\sigma_{y1}^2 + \sigma_{y2}^2)\cos^2\theta + (\sigma_{x1}^2 + \sigma_{x2}^2)\sin^2\theta}}$$

$$\sigma_{Vy} = \sqrt{\frac{(\sigma_{y1}^2 + \sigma_{y2}^2)(\sigma_{x1}^2 + \sigma_{x2}^2)}{(\sigma_{x1}^2 + \sigma_{x2}^2)\cos^2\theta + (\sigma_{y1}^2 + \sigma_{y2}^2)\sin^2\theta}}$$

where θ is the angle between scan axes and principal axes of the beam ellipse. For small eccentricity $\epsilon^2 = 1 - \frac{\sigma_{Vy}^2}{\sigma_{Vx}^2}$ and small θ approximation, the correction to the luminosity calculation is

$$C_{axis} = 1 - (\epsilon \times \theta)^2 \tag{14}$$

This can be used to estimate the error due to the scan axes not being aligned with the beam ellipse or the principal axes not being orthogonal.

III. VAN DER MEER SCAN AT STAR IP AT RHIC

From Eq.6, we know that we have to measure beam currents (N_1, N_2) and beam profiles $(\sigma_{Vx}, \sigma_{Vy})$ for a certain number of bunches k_b in the beam. The total beam intensity is measured by very sensitive "DC" transformer and bunched beam intensity is measured with a wideband wall current pickup [8,9]. The beam profile is measured by van der Meer Scan described in the previous section. There are several methods of measuring the beam profile besides Vernier Scan, such as a rotating wire device [8], STAR tracking vertex which will be discussed in this report as well. However, the Vernier Scan yields the best resolution.

There is at least one Vernier scan carried out for each IP [9]. At STAR IP, we have three very carefully measured scans. For each set position, we recorded beam intensities of both beams, ZDC counts averaging over one minute and the time of the measurement. The three scans are Vernier1 (Aug. 25, 6:00PM→7:42PM), Vernier2 (Aug. 30, 1:20AM→2:30PM) and Vernier3 (Aug. 30, 5:00AM→6:25AM).

A scan was performed by setting the correcting magnet to steer the beam to desired position [8,9]. The set position and the measured position are well calibrated as shown in Fig 1. This has resolution in the order of $10\mu m$. The linearity is better than 99.9% over a large range. The calibration has factors of 0.973 and 0.972 in horizontal and vertical directions which yields an overall correction factor of 1.06 (TableII) to the final absolute cross section. The noise level of the beam current is at a very low level of $2\mu A$ which is much less than 1% of the beam current. The calibration of beam current to number of beam particles is better than 2% in error [9].

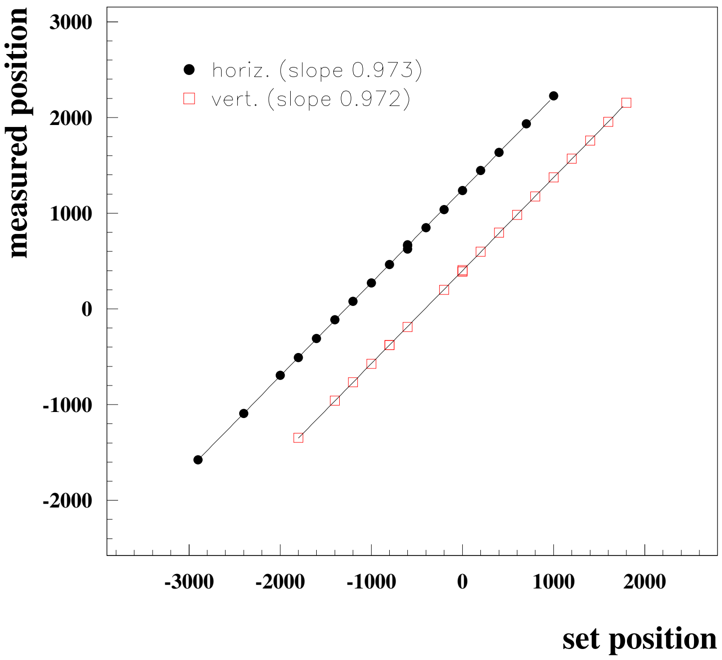

FIG. 1. RHIC beam position calibration in units of μm. Corrections of 0.973 and 0.972 are made to the coordinate scale of the beam profile measurements.

Because the beam intensities in both Blue and Yellow rings decrease as function of time, we normalize the ZDC counts with the beam intensities as $N_{ZDC}/(N_1N_2)$ to cancel out this effect. The absolute cross section then reads as:

$$\sigma_{Au+Au} = (\frac{N_{ZDC}}{N_1N_2})\frac{2\pi\sigma_{Vx}\sigma_{Vy}}{f_{rev}\,k_b} \tag{15}$$

The maximum value of normalized ZDC counts are taken from the fitted constant of the Gaussian fit to the vertical distributions as shown in figures and table which assumes that the horizontal beam overlapping is at its maximum. Correction can be made after the fitting in horizontal distribution to adjust the normalized ZDC count to its maximum using Eq.8. The scan distributions are very Gaussian with good χ^2 which justifies the use of fitted constants as maximum ZDC counts.

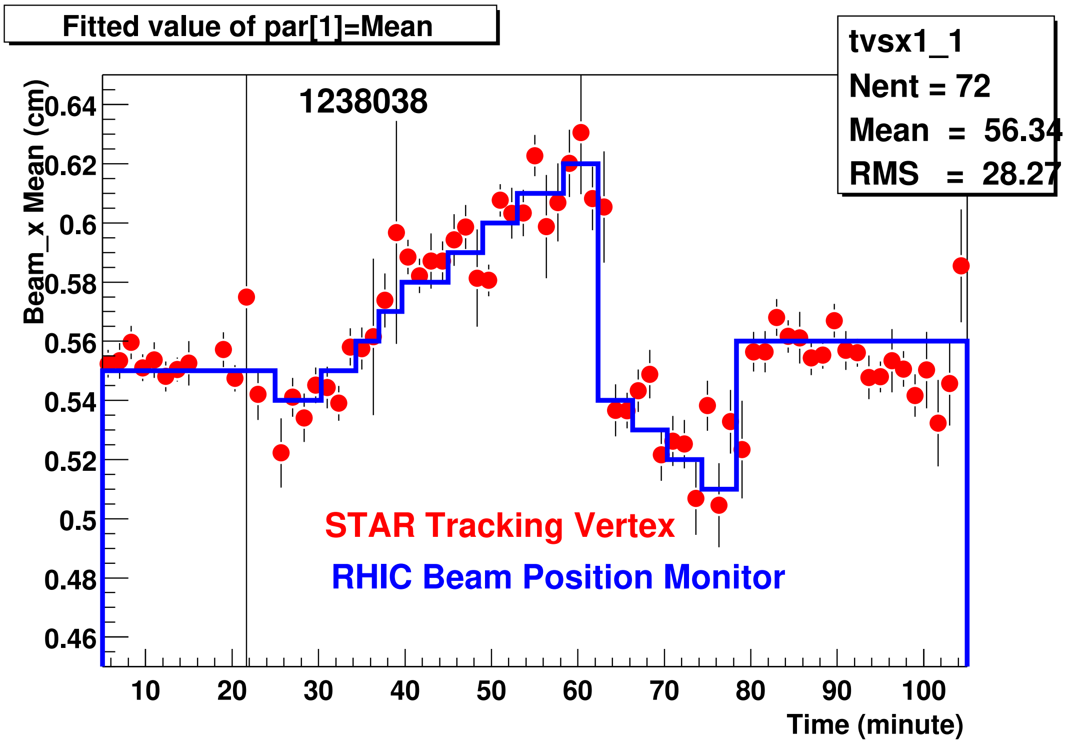

FIG. 2. RHIC predicted beam set position and mean of STAR tracking primary vertex. The horizontal axis is time in units of minutes of the operation and vertical axis is mean value of two-beam overlapping region in units of cm. The agreement between these two is considered to be very good.

During the process of van der Meer Scans, STAR recorded events to tapes as well. Fig.2 shows the good agreement between RHIC beam set position and STAR tracking vertex mean distribution. The scan was done by displacing Blue beam and we correlate the beam position and mean of the STAR tracking primary vertice by scaling $d/2$ according to Eq.13. This also indicates that the beam sizes of both beams are very close to each other.

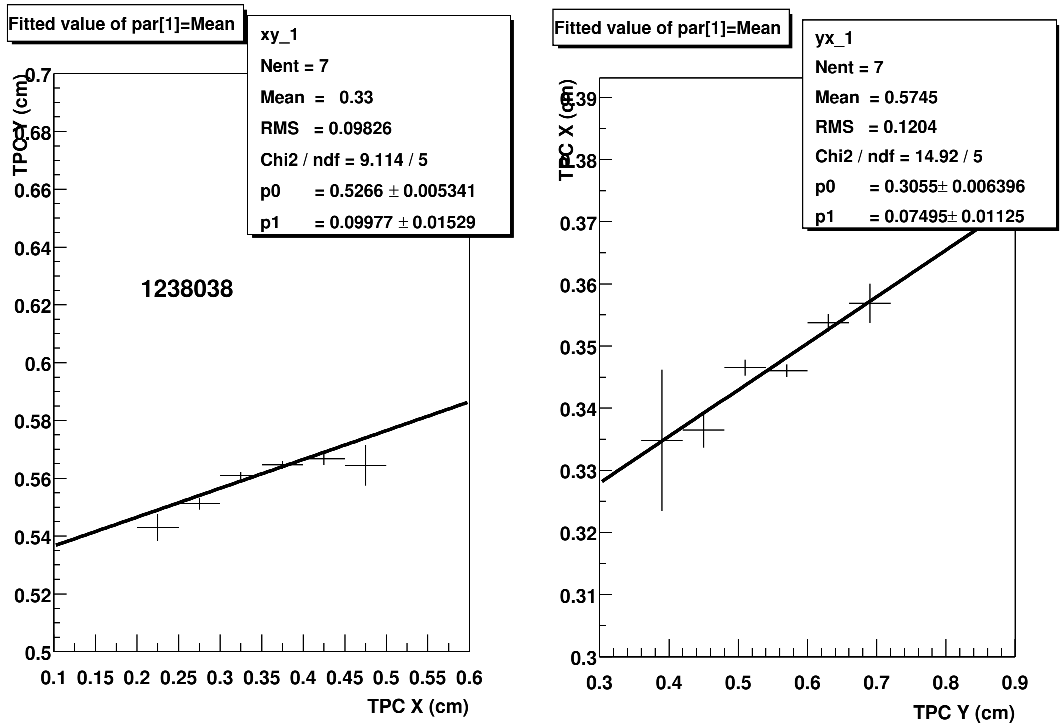

FIG. 3. TPC x vs y distribution (mean value) of beam vertex (tracking primary vertice). This indicates that the principal axes of the beam ellipse and the STAR Coordinate System are not aligned. Under this assumption, we get $\theta \simeq 0.087$.

However, we find that there is small correlation between horizontal and vertical positions from STAR tracking as shown in Fig.3. If we assume that it is due to the misalignment between the principal axes of the beams and the scan coordinates, we get $\theta \simeq 0.087$ for Eq.14. In the three scans we have, the systematics due to this effect are 0.2%, 0.1% and 0.2% respectively according to Eq.14.

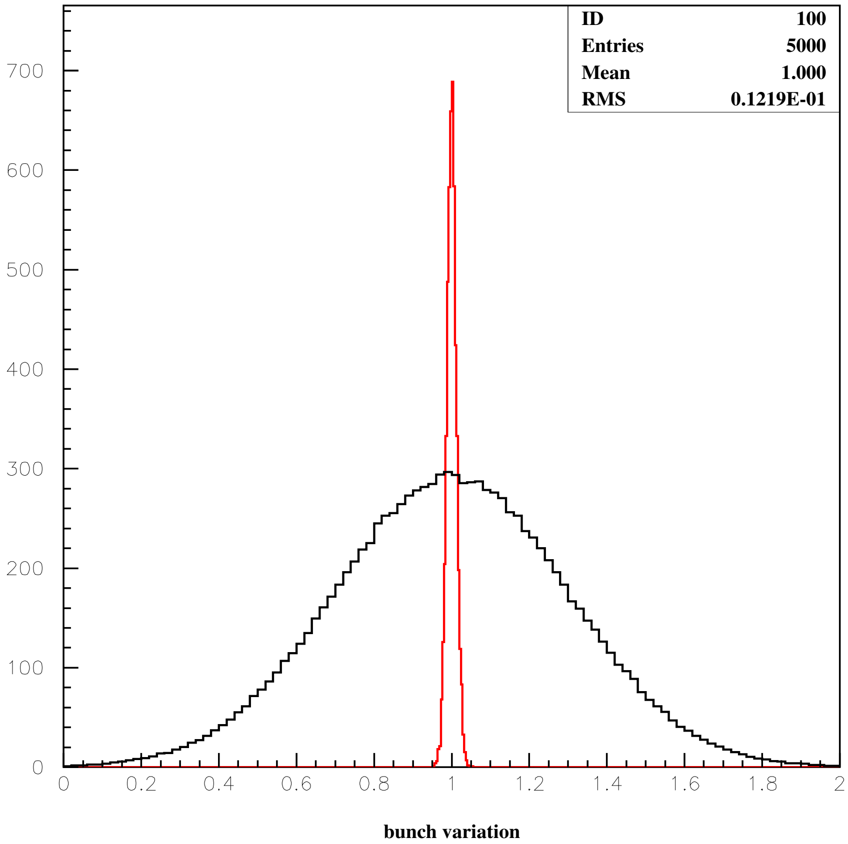

FIG. 4. Individual bunch varies less than 30% overall. Simulations are used to set different conditions of bunch variations of the 55 bunches in both Blue and Yellow beams according to the record in MCR log book. Wide histogram represents the variation of individual bunches and narrow histogram is the result of the uncertainty of cross section calculation from that bunch variation. Bunch variation contributes to uncertainty of about 1% in cross section calculation.

At RHIC, there are 55 bunches in each ring. The intensity is different from bunch to bunch and different in different stores depending on AGS beam availability and details of the injection. Therefore, the difference between product of two total beam intensities $\Sigma N_{1i} \times \Sigma N_{2j}$ and sum of the product of individual bunches $\Sigma(N_{1i}N_{2i})$ has to be investigated. Individual bunched intensity varies less than 30% overall. Simulations are used to set different conditions of bunch variations of the 55 bunches in both Blue and Yellow beams according to the record in MCR log book. Bunch variation contributes to uncertainty of about 1% in cross section calculation under the extreme condition of missing several bunches or 30% variation in beam intensities of individual bunch (see Fig.4).

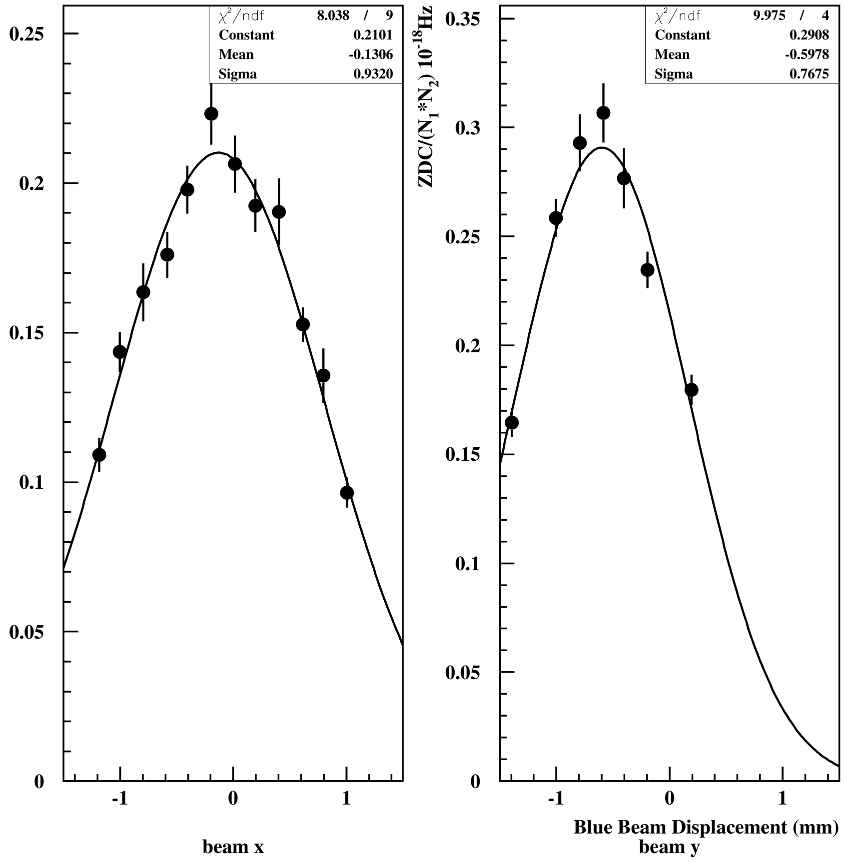

FIG. 5. Normalized ZDC counts as function of beam set position in horizontal and vertical directions for Scan done in Aug. 25 (6:00PM→7:40PM) which is called Vernier1. See text for details.

Scan was done along one direction (Negative X first, then Positive X, then Negative Y and finally Positive Y) so that the effect of the expansion of the beam [8] can be minimized. The expansion of beam can be seen from the beam profile changes from the beginning of the store to the end of the same store in Vernier2 and Vernier3. This measurement justifies the prediction of beam expansion due to intra-beam scattering [8]. If we take the worst case of horizontal scan and use linear extrapolation of beam expansion during the scan to recalculate the normalized ZDC counts, the fitted Gaussian width increases by 0.2% compared to the one without this adjustment, which is negligible at the accuracy of a few percent we are after. Therefore, the final results are presented without this correction. Instead, systematic error of 0.2% is applied to the cross section calculation.

When Blue beam was steered off by as much as 3mm to study to beam-gas background after Vernier2, the ZDC coincidences rate is about 0.2Hz which sets the maximum beam-gas background to be less than 0.3%. In other runs, background may be different because the beam-gas event rate scales linearly with beam intensity but real Au+Au interaction rate goes quadratically.

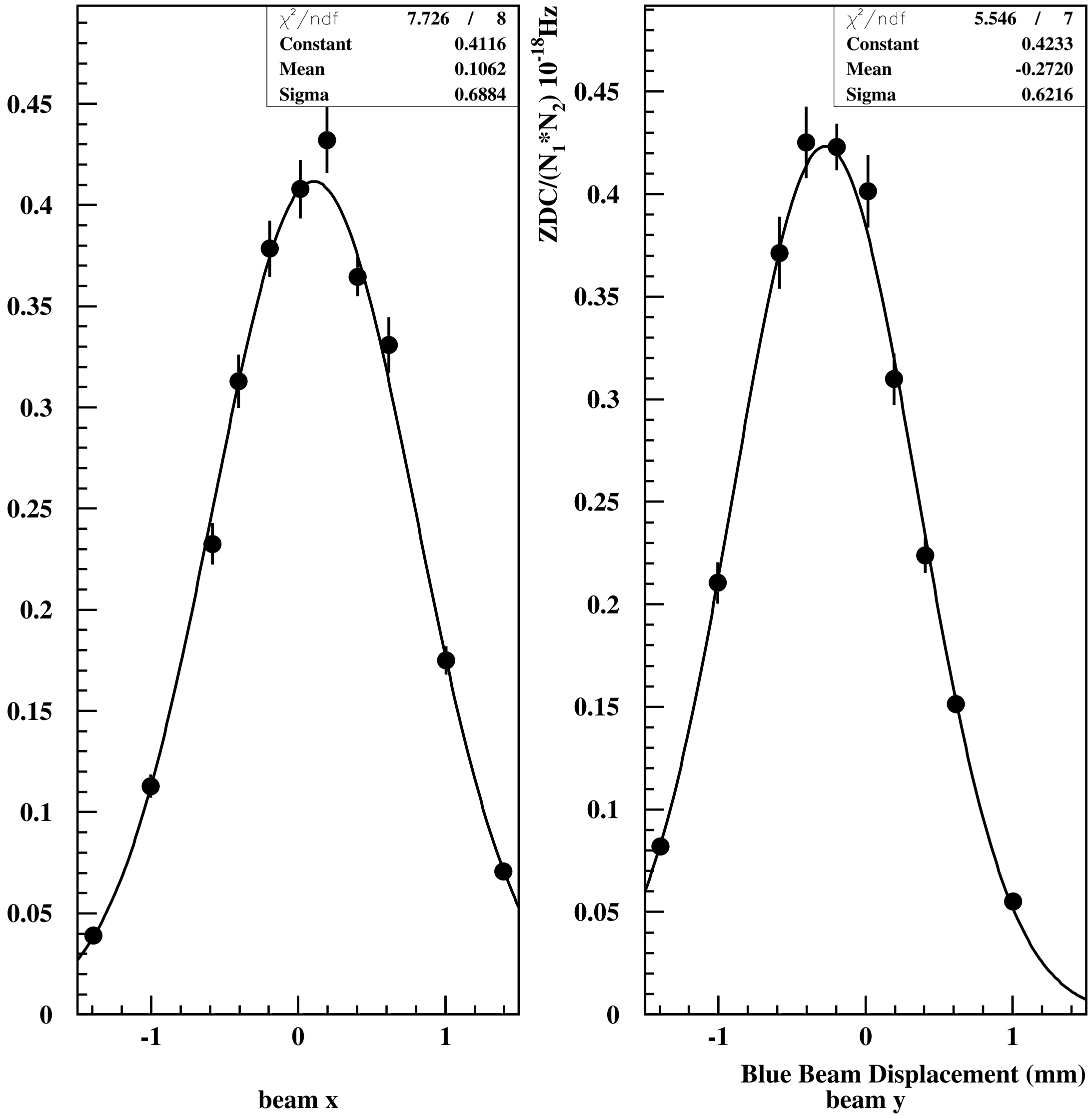

FIG. 6. Normalized ZDC counts as function of beam set position in horizontal and vertical directions for Scan done in Aug. 30 (1:30AM→2:30AM) which is called Vernier2. See text for details.

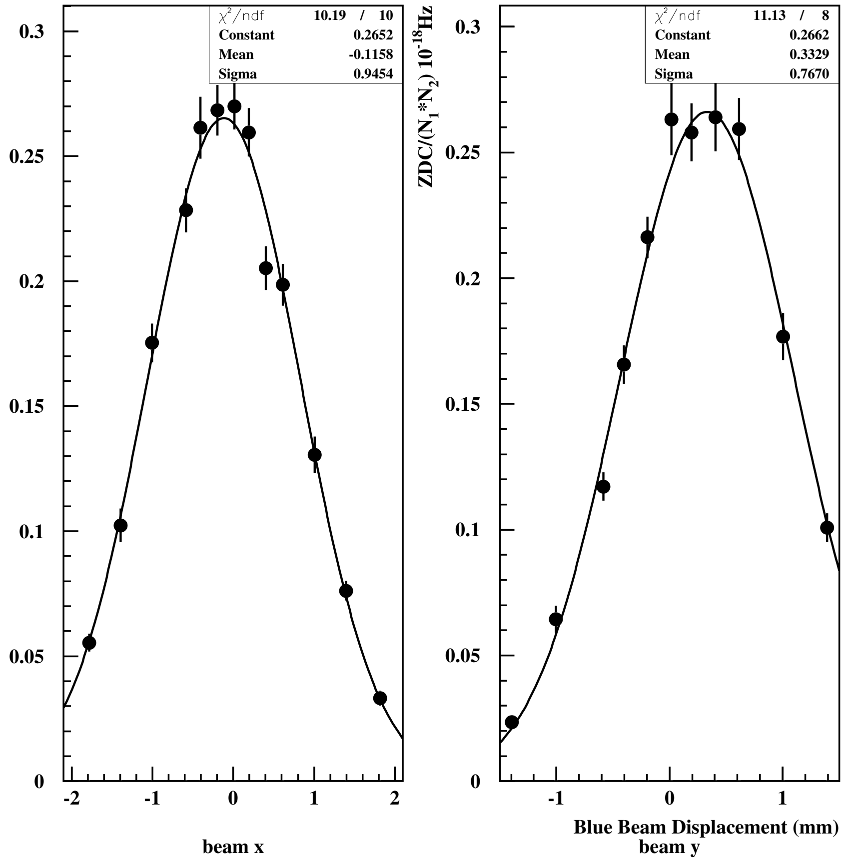

FIG. 7. Normalized ZDC counts as function of beam set position in horizontal and vertical directions for Scan done in Aug. 30 (5:00AM→6:25AM) which is called Vernier3. See text for details.

TABLE I. List of three Van der Meer Scans at STAR IP. The numbers are presented from the fits from plots without any corrections. Corrections and errors are in other tables. See text for details.

Date	$N_{ZDC}/(N_1N_2)(\times 10^{-18}Hz)$	$\sigma_{Vx}(\mu m)$	$\sigma_{Vy}(\mu m)$	Cross section σ_{Au+Au}(barn)
Vernier1	0.291	932	768	9.22
Vernier2	0.423	688	622	8.02
Vernier3	0.266	945	767	8.54

Results of the normalized ZDC counts, beam profiles and cross sections are listed in Table I. Vernier2 and Vernier3 were carried out with the same beam store with Vernier2 at the beginning of the store and Vernier3 at the end of the store. Beam expansion in both horizontal and vertical directions are obvious, especially in horizontal direction. This means that beam profile from any scan should be used ONLY for the luminosity calculation at the time the beam profile is measured. Corrections are made for horizontal off-peak displacement and set position calibration. Final result averaging over three scans weighted by statistical errors is 8.9$\pm$0.34($stat$)$\pm$0.51(sys)(barn). Error analysis (χ^2) of the consistency of these three results shows Confidence Level of 90%. Systematic and statistic errors of the scans are studied in details as shown in Table III. Because statistical errors are derived from the same Gaussian fits to the scan distribution, they are added linearly. Systematic errors are added linearly as well. If we add the total statistical and total systematic errors quadratically, we have 8.9barn $\pm$6.8%

TABLE II. Corrections are made for horizontal off-peak displacement and set position calibration. Final result averaging over three scans is 8.9$\pm$0.34($stat$)$\pm$0.51(sys)(barn). Error analysis (χ^2) of the consistency of these three results shows Confidence Level of 90%.

Date	Beam centering in X (μm)/correction	scale of set position	Corrected σ_{Au+Au}(barn)
Vernier1	70/1.003	1.06	9.8
Vernier2	94/1.009	1.06	8.6
Vernier3	95/1.005	1.06	9.1

TABLE III. Systematic and statistical errors of the scans. Systematic and statistical are added linearly respectively. If we add the total statistical and total systematic errors quadratically, we have 8.9barn $\pm$6.8%

Date	$N_{ZDC}/(N_1 N_2)$	σ_{Vx}	σ_{Vy}	total statistic error	bunch variation	axis alignment	beam expansion	beam current calibration	beam-gas background	total systematics
Vernier1	2.2%	3.%	3.7%	9.%		0.2%				
Vernier2	1.7%	1.0%	0.8%	3.5%	1.%	0.1%	0.2%	2.%+2.%	0.3%	5.7%
Vernier3	2.1%	1.3%	1.9%	5.%		0.2%				

IV. APPLICATIONS

In this section, we will try to have a rough comparison with theoretic prediction and demonstrate the procedure of applying this measurement of absolute cross section to normalize the minimum bias distribution of $d\sigma_{Au+Au}/dN_{ch}$. Detailed studies of ZDC and unnormalized multiplicity distribution can be found elsewhere [10,11].

The measured $8.9 \pm 0.34(stat) \pm 0.51(sys)$(barn) is the absolute cross section of Au+Au interaction at $\sqrt{s_{NN}} = 130GeV$ seen by the ZDC coincidences located about 18 meters in both EAST and WEST of the IP. This cross section includes mutual Coulomb dissociation and minimum bias nuclear interaction which generate single or multiple neutrons in forward direction. The cross section predicted [2] is 10.9barn at $\sqrt{s_{NN}} = 200GeV$ and small energy dependence brings the cross section down to 10.75 barns [12] at $\sqrt{s_{NN}} = 130GeV$. If we add all the errors including uncertainty in theoretical prediction quadratically, we see two-sigma difference between measured and predicted values. If the errors are added linearly, we have 1.2σ difference. If we require that there is at least one CTB (Central Trigger Barrel) hit to be called a nuclear interaction, $67 \pm 3.4\%$ of the total cross section seen by ZDC coincidences [10] is from nuclear interactions. So the nuclear cross section seen by ZDC coincidences from these measurements is $8.9 \times 67\% = 6.0 barn$. The total nuclear cross section at AGS energies was measured to be about 6.5barn [13]. Interactions which have only charged particles [13,14] in final state , such as 1 proton event, proton photodissociation, proton pickup or large fragmentations, can not be detected and triggered by ZDC coincidences. The fraction of $\sigma_{(1n,1n)}$ predicted by theory [2] is 4.1% while the measurement is 5.% [10]. If we assume that the increase of the fraction of (1n,1n) cross section is due to the fact that ZDC can not trigger on (inefficiency) the interactions with all charged particles in final state, then the predicted cross section seen by ZDC will be $\frac{4.1\%}{5.\%} \times 10.75 = 8.8$barns which is consistent with the measured 8.9barns.

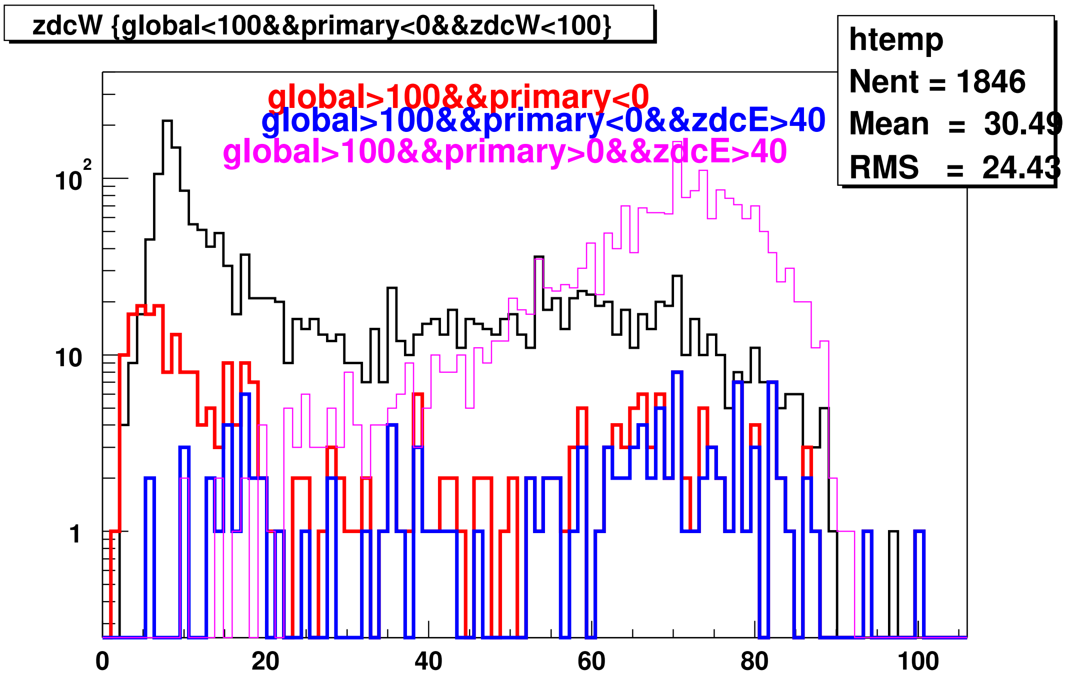

FIG. 8. ZDC West distribution for different cuts! See text for details.

There are several issues which make the normalization of multiplicity distribution nontrivial. For example,

- most of the Coulomb dissocation interactions do not leave anything in CTB, therefore, we can not reconstruct the event in TPC,
- the interaction diamond extends out of TPC in beam direction,
- beam-gas event rate changes from run to run,
- there is inefficiency in vertex finding at low multiplicity.

First, we investigate the beam-gas background in runs 12280xx from which the multiplicity distribution is to be produced. The attenuated ADC counts of ZDC WEST signals are shown in Fig.8 for different cuts.

- $(global < 100\&\&primary < 0)$ means there are less than 100 global tracks in the event without primary vertex. This represents interactions with large impact parameter or Coulomb Dissociation.
- $(global > 100\&\&primary < 0)$ represents beam-gas events and Au+Au interactions occurring outside TPC fiducial volume.
- $(global > 100\&\&primary < 0\&\&zdcE > 40)$ largely represents Au+Au interactions occurring outside TPC fiducial volume.
- $(global > 100\&\&primary > 0\&\&zdcE > 40)$ represents Au+Au interactions with small impact parameter.

Justification of the representations is that the zdcW distributions are what one would expect in all the cases. The beam-gas events are estimated to be about 3%.

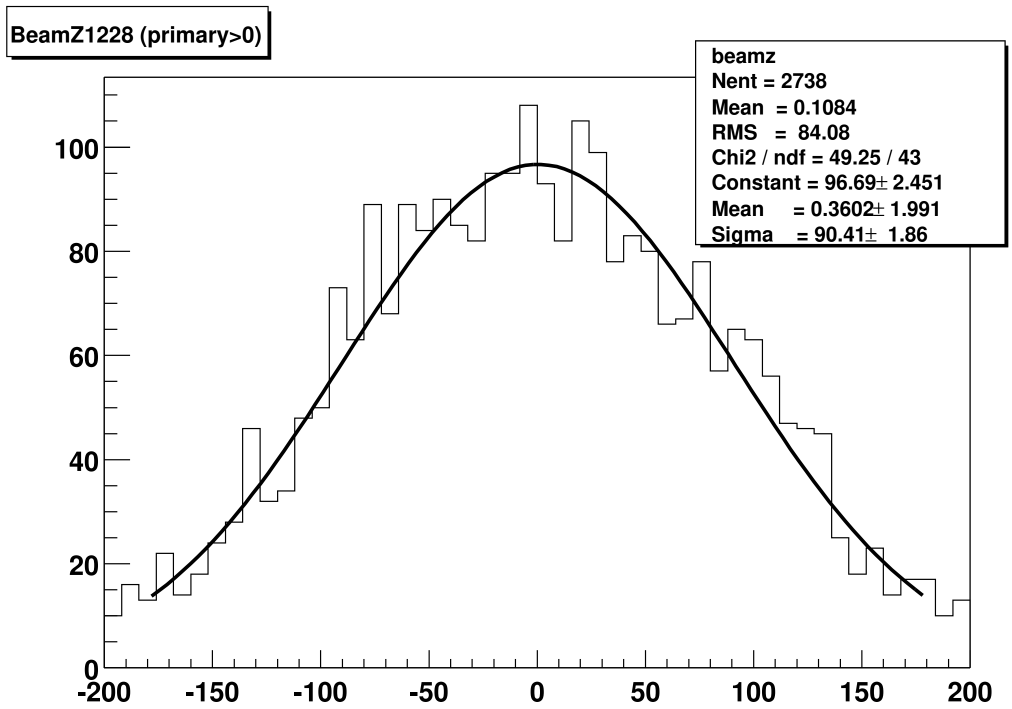

FIG. 9. Interaction diamond distribution along beam direction. TPC fiducial volume is $|z| < 200cm$. With a vertex cut of $|z| < 95cm$, about 70% of the interactions occur inside of this cut.

The other item we need to know is the fraction of the total number of events we analyze which is relevant to the total cross section. Fig.9 shows that about 70% of the interactions occur inside the region with $|z| < 95cm$ which is the vertex cut in dN/dN_{ch} analysis [11]. (Only less than 70% of the events occur inside this region can be reconstructed with good primary vertex definition.) This study assumes the event reconstructing efficiency does not change much as function of interaction position in TPC. More detailed studies of vertex efficiency and beam-gas events are in [10,11,16]. Now, if we have the dN/dN_{ch} from total number of events N_{total} recorded in tape with minimum bias trigger (ZDC trigger), we can normalize it as follows:

$$\frac{d\sigma}{dN_{ch}} = \frac{8.9}{97\% \times 70\% \times N_{total}} \frac{dN}{dN_{ch}} (barn) \tag{16}$$

In summary, the total cross section of Au+Au at $\sqrt{s_{NN}} = 130GeV$ is determined to be $8.9 \pm 0.34(stat) \pm 0.51(sys)$(barn) by van der Meer scan. Next year, RHIC will run at $\sqrt{s_{NN}} = 200GeV$ which will allow us to study the energy dependence of the cross section. Most of the systematic errors will cancel out when we take the ratio and we expect to have total statistical error of about 4% which is largely from this year's statistical error.

V. ACKNOWLEDGEMENTS

We wish to thank the RHIC Operations Group at Brookhaven National Laboratory for their tremendous support and for providing collisions for the experiment. The authors would like to thank T. Satogata, J. Jamilkowski of the RHIC Operations Group for carrying out the Vernier Scan and C. Adler, B. Christie, H. Crawford, J. Harris, P. Jacobs, D. M. Reichhold, T. Trainer, T. Ullrich, J. Westfall for discussions and coordinating the activities. This work was supported by the Division of Nuclear Physics and the Division of High Energy Physics of the Office of Science of the U.S. Department of Energy.

[1] J. Schukraft, the 19th Symposium on Multiparticle Dynamics, Arles, France, 13-17 June 1988; KEK88-10-390.
[2] A. Baltz, et al., Nucl. Instr. and Method, A417 (1998) 1
[3] C. Adler, et al., nucl-ex/0008005.
[4] S. van der Meer, ISR-PO/68-31, KEK68-64.
[5] G. Giacomelli and M. Jacob, Physics Report, 55 (1979)1.
[6] P. Bryant and K. Potter, CERN-ISR-ES-BOM/82-15, KEK83-1-138.
[7] P. Castro-Garcia, CERN SL/96-70, KEK97-01-158.
[8] Conceptual Design of RHIC, May, 1989; http://www.agsrhichome.bnl.gov/NT-share/rhicdm/00_toc1i.htm
[9] A. Drees, et al., RHIC note (in preparation).
[10] C. Adler, et al., STAR note (in preparation).
[11] M. Calderon de la Barca Sanchez, et al., STAR note (in preparation)
[12] S. White, C. Adler, private communications.
[13] C.J. Waddington, et al., Phys. Rev. C, 61 (2000) 024910; L.Y. Geer, et al., Phys. Rev. C, 52 (1995) 334
[14] J. Barrette, et al., Phys. Rev. C, 41 (1990) 1512
[15] K.H. Ackermann, et al., nucl-ex/0009011
[16] P. Jacobs, J. Castillo, et al., starsoft-l@bnl.gov and private communication